

Preparation of the Flexible Polypyrrole/Polypropylene Composite Fibrous Film for Electrochemical Capacitor

Ming Jin, Yanyun Liu, Yulin Li, Yunzhen Chang, Dongying Fu, Hua Zhao, Gaoyi Han

Institute of Molecular Science, Key Laboratory of Chemical Biology and Molecular Engineering of Education Ministry, Shanxi University, Taiyuan 030006, People's Republic of China

Received 5 January 2011; accepted 24 February 2011

DOI 10.1002/app.34438

Published online 12 July 2011 in Wiley Online Library (wileyonlinelibrary.com).

ABSTRACT: Polypyrrole (PPy)/polypropylene fibrous membrane (PPF) composite materials with different PPy contents are prepared through *in situ* chemical oxidation polymerization in the pyrrole atmosphere at room temperature by dissolving the $\text{FeCl}_3 \cdot 6\text{H}_2\text{O}$ in methanol and acetonitrile as oxidant. The morphology of the composite is examined by scanning electron microscope (SEM), the conductivities of the composites are measured by convenient four-probe method, and the properties of the capacitor cells assembled by the obtained PPy/PPF are investigated by cyclic voltammetry (CV), galvanostatic charge/discharge, and electrochemical impedance spec-

troscopy (EIS) measurements. The results show that the morphology, conductivity, and the capacitor property of the composite are influenced strongly by the solvent of the oxidant. The capacitor assembled by the PPy/PPF prepared by using acetonitrile as the solvent for $\text{FeCl}_3 \cdot 6\text{H}_2\text{O}$ can adapt for quick charge/discharge, and exhibit the highest capacitance of about 72.5 F g^{-1} when the PPy content is about 8.0%. © 2011 Wiley Periodicals, Inc. *J Appl Polym Sci* 122: 3415–3422, 2011

Key words: conducting polymers; polypyrrole; polypropylene; electrochemistry; capacitor

INTRODUCTION

Supercapacitor, also called electrochemical capacitor, is a kind of new energy storage system as compared with normal capacitor and battery, and an important object of science and industrial development during the last years.^{1–5} Based on the charge storage mechanism, electrochemical capacitor is classified into two categories: one is the electrical double-layer capacitor which utilizes mainly the separation of electronic and ionic charges at the interface between electrode materials with large-surface area and the electrolyte solution^{6,7}; the other is the pseudocapacitor which is based on the Faradaic redox reactions occurring within the active electrode materials.^{8,9} Recently, a great interest has focused on the development of thin, flexible, lightweight, and environmentally benign electrochemical capacitor to meet the various requirements of modern gadgets,^{10–12} which requires

the novel conducting composites to be used as the electrode materials. So the choice of the component of the composites and the manufacturing technology becomes a crucial factor for developing the effective electrode materials.

Comparing with activated carbon¹³ and transition metal oxides,^{14–19} conducting polymers studied widely such as polyaniline (PANI), polypyrrole (PPy), and polythiophene (PTH) have attracted great interest for being candidates in fabrication of various electronic devices^{20–23} because of their various structures and high conductivity. Among the conducting polymers, PPy has attracted much attention owing to its unique electrical conductivity, redox property, and excellent environmental stability.^{24–27} Up to date, various polymerization methods including polymerization in solution,²⁸ in vapor phase^{25,26,29} and under supercritical conditions³⁰ have applied to prepare the PPy with various microstructures. In the past, many attempts have been tried to produce energy storage devices consisting of entirely nonmetal components. One method for improving the flexible electrode based on the conducting polymer is related to the use of nonmetal substrates for polymer deposition, which can combine the properties of the constituents and make it possible to overcome the drawbacks of the individual materials.^{31–34} Recently, the electrodes based on the composite of PPy have been fabricated by depositing PPy on the nonmetal substrates with larger surface area such as the carbon fibers, celluloid and polysaccharide fibers,

Correspondence to: G. Han (han_gaoyis@sxu.edu.cn).

Contract grant sponsor: National Natural Science Foundation of China; contract grant numbers: 21073115, 20604014.

Contract grant sponsor: Program for new century excellent talents in university (NCET) of China.

Contract grant sponsor: Program for the Top Young and Middle-aged Innovative Talents of Higher Learning Institutions of Shanxi province (TYMIT and TYAL).

and at the same time the performance of the capacitor prepared by the composites have also been evaluated.^{35–42}

Polypropylene fibrous membrane (PPF) is an interesting substrate material as compared with the other nonmetal substrates because of its relatively high surface-to-mass ratio, good mechanical property and flexibility, chemical resistance, and the ability to be shaped in various forms. In this article, we present a simple and convenient route to directly fabricate PPy/PPF composite which fits the characteristics of capacitor electrode and provides inherent flexibility as well as porosity via an *in situ* vapor phase polymerization method. Thus, the obtained PPy/PPF composites can be not only lightweight, flexible enough to be rolled up or twisted, and also manufactured at low cost.

EXPERIMENTAL

Materials

Methanol, acetonitrile, anhydrous alcohol, potassium chloride, ferric chloride hexahydrate ($\text{FeCl}_3 \cdot 6\text{H}_2\text{O}$) were analytical grade and used without further purification. Pyrrole was distilled under reduced pressure before use and stored at a temperature less than 5°C. The polypropylene fibrous mats (PPF) formed by PP fibers with many pores and a thickness of 450 μm was purchased from Cullender Factory of Guodian.

Preparation of flexible PPy/PPF composites

The flexible PPy/PPF composite materials were prepared by using ferric chloride as the oxidant to react with the pyrrole vapor in an airtight vessel at room temperature. The methanol and acetonitrile were used as the solvent of ferric chloride. In a typical process, different amounts of ferric chloride are dissolved into the solvent to form various concentrations solution (50, 100, 150, 200, 250, 300, and 350 g L^{-1}), then the PPF films are soaked in the solution for 3 min. When the excess solution was eliminated by a filter paper, the PPF films adsorbed with oxidant were suspended in a sealed vessel containing pyrrole vapor at room temperature. After 72 h, the obtained black PPy/PPF composite films were dipped into ethanol several times to remove the impurity. Finally, the product was dried in vacuum at room temperature for 10 h. The content of the PPy in the composites was determined by measuring the weight of the composites and PPF. The PPy/PPF composites prepared by using methanol and the acetonitrile as oxidant solvent were named as M-PPy/PPF and A-PPy/PPF, respectively.

Characterization

The morphologies of the PPy/PPF composites were measured by using a scanning electron microscope (SEM, JEOL 6701), and the samples were sputtered with platinum before observation. The *dc* electrical conductivities were measured using the standard four-probe technique, where the conductivity (σ) can be defined as follows eq. (1):

$$\sigma = IL/VS \quad (1)$$

where I , V , and L were defined as the applied current, the output voltage and the length of samples between the two inner electrodes, respectively, and the S was the sectional area of the samples.

The capacitor cells were assembled by using two pieces of PPy/PPF composite films (one oxidized and one reduced) as the two electrodes, a filter paper soaked with 1.0M KCl is used as the electrolyte to separate the two pieces of PPy/PPF films. Two platinum foils contacted with the films were used as the current collectors while two pieces of PVC plate were utilized to coat and stabilize the cell. All the electrochemical measurements were carried out on a CHI 660C electrochemical station by using double-electrode technique. The cyclic voltammetry (CV) measurements were performed in a voltage range of -0.5 to 0.5 at different scan rates. Galvanostatic charge/discharge measurements were performed at varying current density with the cutoff voltage of -0.5 and 0.5 V. The electrochemical impedance spectroscopy (EIS) measurements were performed at open-circuit potential and the data were collected in the frequency range of 0.01 – 10^5 Hz with AC-voltage amplitude of 5 mV.

RESULTS AND DISCUSSION

Morphology and conductivity

The morphology of primordial PPF membrane is shown in Figure 1(a), from which we can see that the surface of the fibers is smooth and the diameter of most PP fibers ranges from 3 to 6 μm except some thick fibers with a diameter larger than 10 μm , the size of the pores dispersed on the surface ranges from several hundred nanometers to several micrometers. Comparing with the PPF [Fig. 1(a)], a great morphology change on the surface of PPy/PPF composite [Fig. 1(b–f) and Fig. 2] takes place, e.g., the surface becomes rough because the PP fibers has been coated with PPy. Furthermore, the morphologies of A-PPy/PPF composites prepared by using acetonitrile as oxidant solvent become more coarse or rugate with the increase of the content of PPy. For example, at low contents (2.8%, 5.7% PPy), a thin PPy layer is observed on the surface of the PP

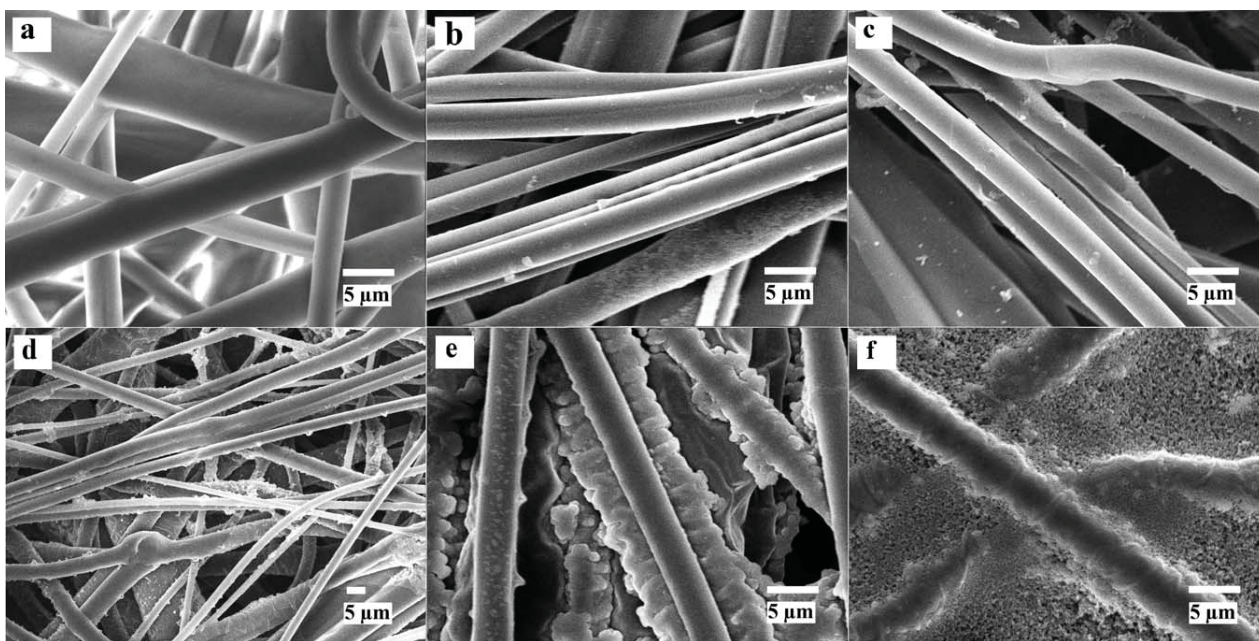


Figure 1 SEM images of pristine PPF film (a), and various contents of PPy in A-PPy/PPF composite: (b) 2.8%; (c) 5.7%; (d) 8.0%; (e) 23.9%; and (f) 48.4%.

fibers [Fig. 1(b,c)]. When the content of the PPy increases to 8.0%, as shown in Figure 1(d), the rugate and coarse layer of polymer is observed on the PP fibers. At higher content of the PPy such as 23.9%, lots of crimples are observed on the surface of PP fibers [Fig. 1(e)], while the content of the PPy increases to 48.4% further, it is found that the pores

dispersed on the surface have been filled with the formed PPy [Fig. 1(f)]. The morphologies of M-PPy/PPF prepared by using the methanol as oxidant solvent are shown in Figure 2, comparing with the Figure 1, the similar phenomena are observed. With the increase of PPy content, the fibers are encased by the formed PPy firstly (from 14.0% to 29.0%) just as

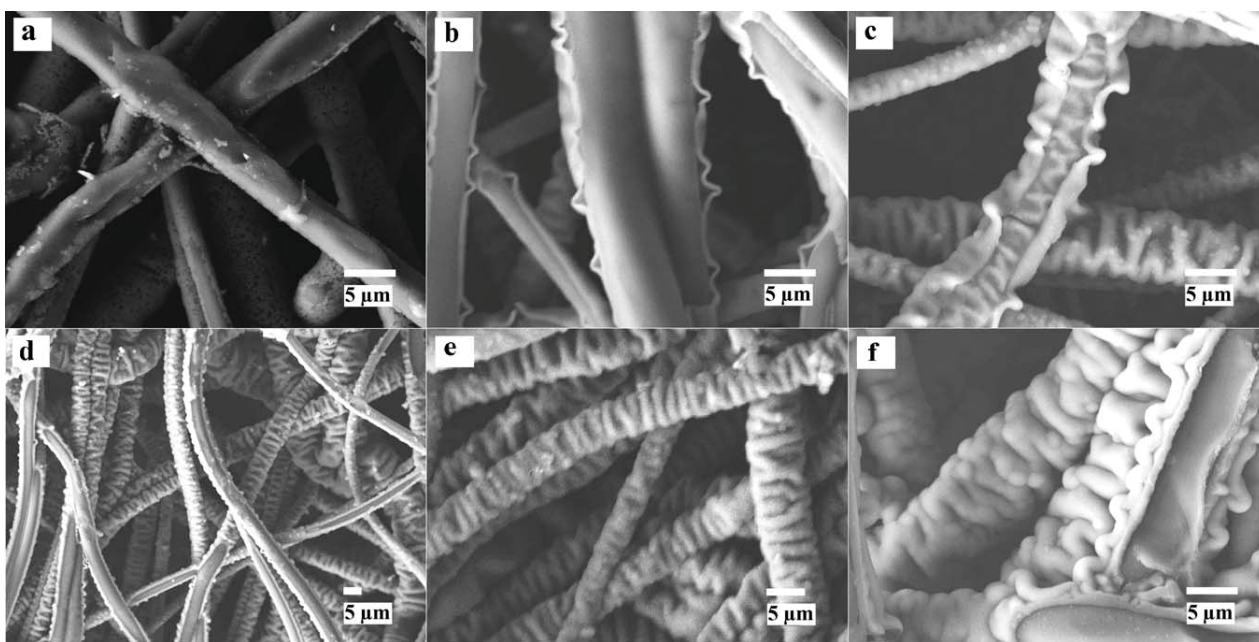


Figure 2 SEM images of various contents of PPy in M-PPy/PPF composite (a) 14%; (b) 19.7%; (c) 29%; (d) 33.4%; (e) 35.1%; and (f) 44%.

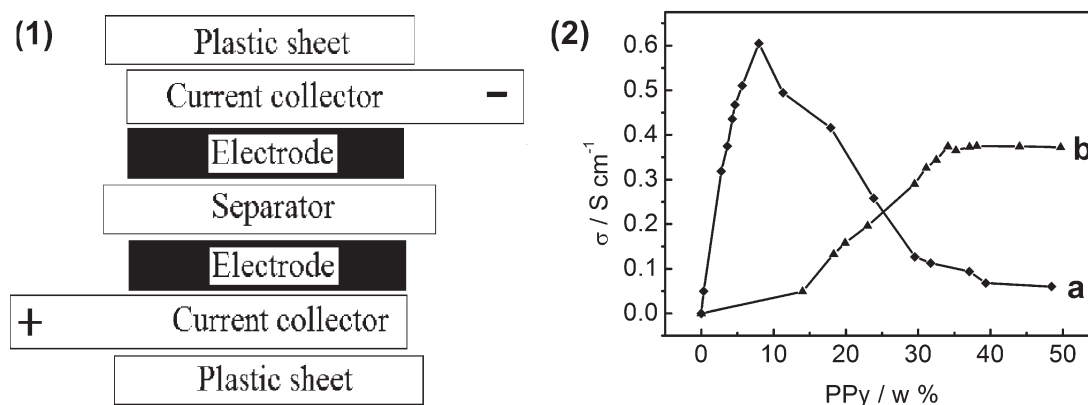


Figure 3 The schematic illustration of the cell (1) and the relationships between the conductivities and the actual PPy contents in PPy/PPF composites (2) at room temperature, curve a is the A-PPy/PPF composite, curve b is the M-PPy/PPF composite.

in Figure 2(a–c). Then a thick and crinkly layer of PPy is deposited [Fig. 2(d–f)], compared with A-PPy/PPF, the pores of the PPF can still be observed when the content of PPy reaches 44.0%.

The conductivities of the composites have been measured based on the convenient four-probe technique and the plot of conductivities versus the PPy content is shown in Figure 3, from which it is possible to observe that the conductivity increases with the augmentation of the PPy content in the initial stage for both kinds of composites. The difference is that the conductivities have almost not changed with the increase of PPy content for M-PPy/PPF after the conductivity reaching the maxim, while dramatically decrease with the increment of content of PPy for A-PPy/PPF [Fig. 3(2)b–a]. The optimum conductivity of A-PPy/PPF reaches 0.61 S cm^{-1} for the sample containing 8.0% PPy, while the maximum conductivity of M-PPy/PPF is 0.37 S cm^{-1} when the PPy content reaches 34.1%. It is well known that the synthesized PPy from nonproton solvent exhibits higher conductivity than that from proton solvent, so the maximum conductivity for A-PPy/PPF is higher than that for M-PPy/PPF. It should be noted that $\text{FeCl}_3 \cdot 6\text{H}_2\text{O}$ exhibits a higher solubility in methanol than that in acetonitrile, so more $\text{FeCl}_3 \cdot 6\text{H}_2\text{O}$ can be dissolved in the methanol completely while not in acetonitrile. In low content of $\text{FeCl}_3 \cdot 6\text{H}_2\text{O}$, the formed PPy enwraps the PP fibers and the conductivity increases with the augmentation of the $\text{FeCl}_3 \cdot 6\text{H}_2\text{O}$ in the acetonitrile, yet, with the content of $\text{FeCl}_3 \cdot 6\text{H}_2\text{O}$ increasing furthermore, the undissolved $\text{FeCl}_3 \cdot 6\text{H}_2\text{O}$ particles disperse between the pores and the fibers, the formed PPy particles contact loosely when the thickness of the composite becomes large dramatically, so the conductivity reaches the maximum and then decreases with the increment of the $\text{FeCl}_3 \cdot 6\text{H}_2\text{O}$. However, $\text{FeCl}_3 \cdot 6\text{H}_2\text{O}$ exhibits high solubility in methanol, the

PPy formed on the surface of the PP fibers although the content of $\text{FeCl}_3 \cdot 6\text{H}_2\text{O}$ in methanol is higher, the thickness of the composite increases with the decrement of the resistance, so the conductivity almost remains constant when the conductivity reaches the maximum.

Electrochemical characterization of the capacitor cells of PPy/PPF composite

Cyclic voltammerty method is used to characterize the capacitor cells assembled by the PPy/PPF composites and the results are shown in Figure 4. From the CV curves, it can be seen that the curves at different scan rates show no redox peaks for A-PPy/PPF and M-PPy/PPF in the whole voltage range during both positive and negative sweeps, indicating that the electrode is charged and discharged at a pseudoconstant rate over the whole CV process, and the shapes of the CV curves are rectangular-like with the almost symmetric I-E responses [Fig. 4(a,b)] when the CV scan rate is lower than 100 mV s^{-1} . This is corresponding to the rapid current response on voltage reversal at each end potential and it is in accord to the ideal capacitive behavior, indicating that the composites can be used as the candidate for electrochemical capacitors. From the figure, it is also found that the CV curves shapes of the cells prepared by A-PPy/PPF show more rectangular-like form than that of M-PPy/PPF, which illustrates that the A-PPy/PPF material exhibits better capacitive property than M-PPy/PPF composite. Furthermore, cells prepared by the A-PPy/PPF retain the rectangular-like CV curves although the scan rate increases to 500 mV s^{-1} . However, the CV curves shape can not keep rectangular-like while the CV scan rate increases to 200 mV s^{-1} for the cell prepared by the M-PPy/PPF. The above results indicate that a very rapid charge/discharge reaction can occur in the A-

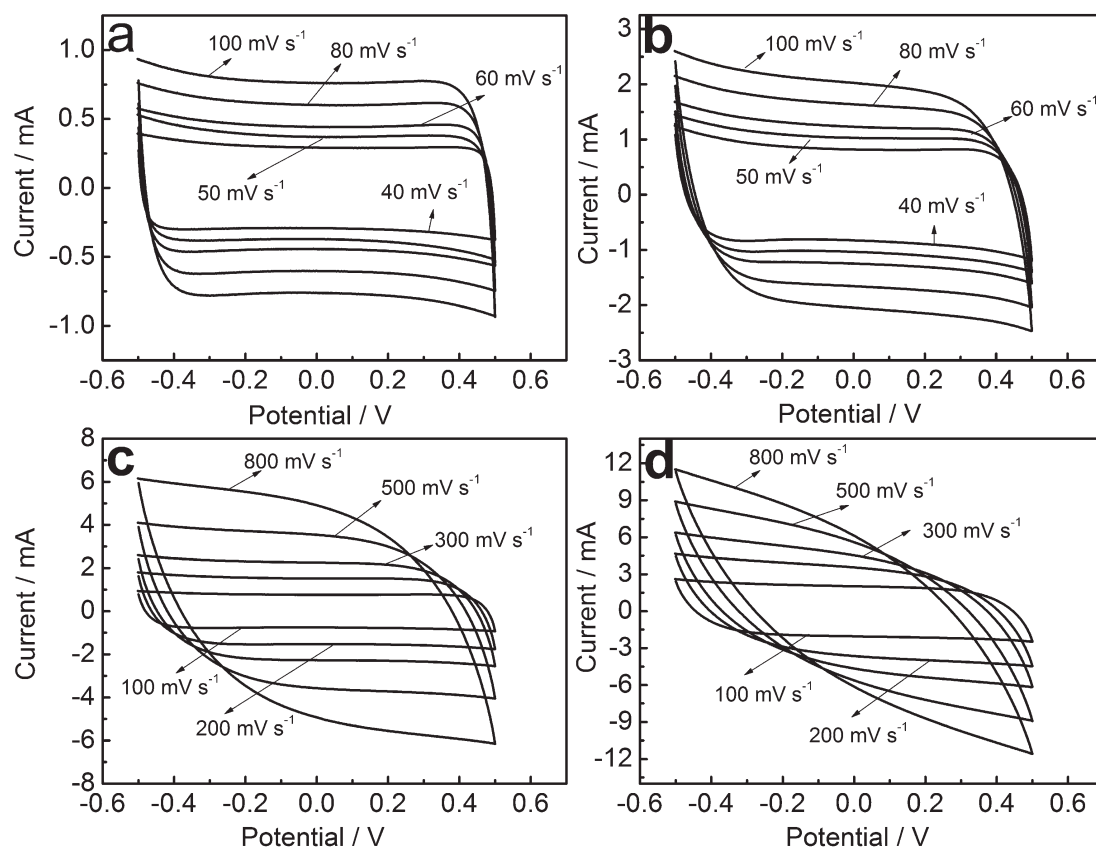


Figure 4 Cyclic voltammograms behaviors of PPy/PPF composite at various scan rates, (a) and (c) are the A-PPy/PPF composite, (b) and (d) are the M-PPy/PPF composite.

PPy/PPF composite because the A-PPy/PPF exhibits higher conductivity and thin layer structures. It is known that the redox reactions occurring on the PPy attend by the doping-undoping counter ion (Cl^-) in the matrix of the conducting polymer from the electrolyte,³³ the diffusion of ions from the electrolyte can access to almost all available space at low scanning rates, leading to a complete insertion reaction. However, with the increase of the scan rates, the effective interaction between the matrix and the electrolyte reduces greatly, the deviation from rectangularity of the CV becomes obvious.

To analyze the variation of capacitance with varying scanning rate, the specific capacitance of the cell can be calculated by eq. (2) based on CV curves.

$$C = Q/V = \int idt/\Delta V \quad (2)$$

where the i is the current, dt is the scanning time span, and ΔV is the total potential range of the voltage window. Figure 5 shows the specific capacitance variations of the cells prepared by using A-PPy/PPF and M-PPy/PPF composites as electrode with scan rate ranging from 40 to 800 mV s^{-1} . It can be seen that A-PPy/PPF composite has a consistent higher

specific capacitance than M-PPy/PPF composite, although the specific capacitances of A-PPy/PPF and M-PPy/PPF composite electrodes all decrease gradually with the increasing scan rate. This result is attributed to the fact that A-PPy/PPF composite has high conductivity and thin layer with the porous structure, which makes the counter ion be easily

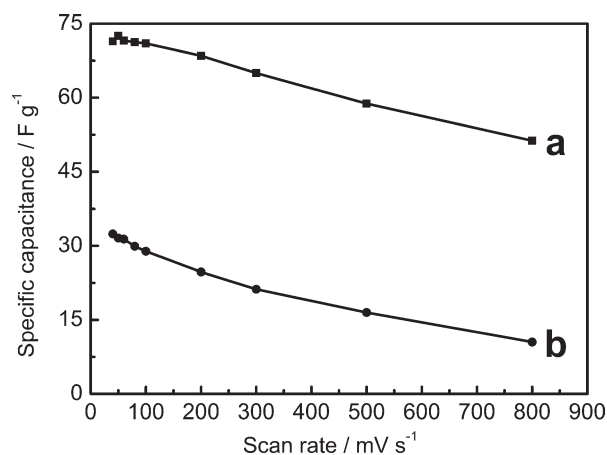


Figure 5 The specific capacitances of the PPy/PPF composite electrodes, a curve is the A-PPy/PPF composite, b curve is the M-PPy/PPF composite.

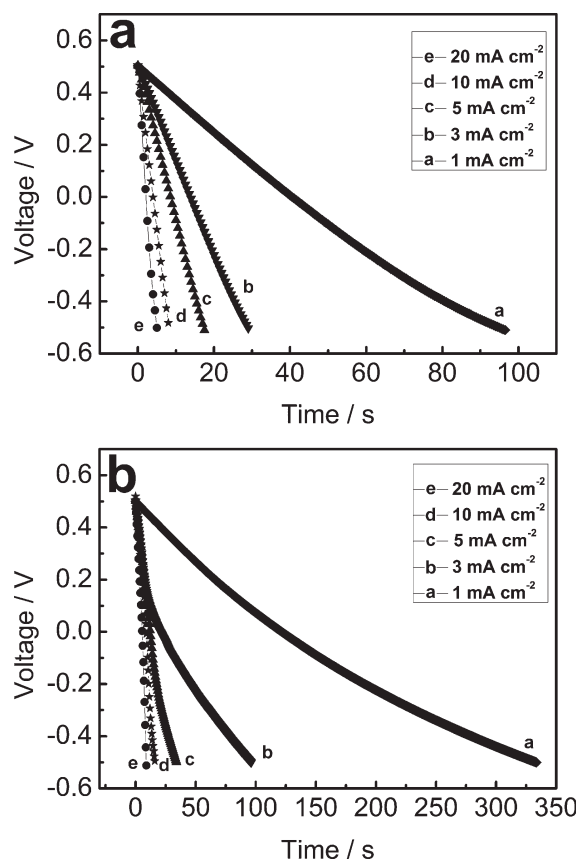
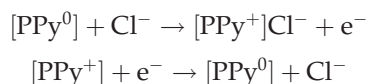


Figure 6 Discharge curves of PPY/PPF composite at various discharge rates: (a) the A-PPy/PPF composite and (b) the M-PPy/PPF composite.

doped and undoped in the matrix of the polymer, and form a large number of electrochemically active sites.

The galvanostatic charge/discharge is also carried out at various rates within the potential between -0.5 V and 0.5 V and the results are shown in Figure 6. The charge/discharge process of the electrochemical redox reaction between the electrode and electrolyte is shown as follows:



For a fully charged state of the cells, the anodic process is neutral because the PPy does not have any n -doping ability. The cathodic process is the fully oxidized state and charge neutrality is maintained by the chloride ions. During the discharge process, the PPy in the cathodic process is reduced and the anode is oxidized to reach the same potential state, and the counter-ions ejected from the cathode are inserted in the anode electrode to maintain charge neutrality. Figure 6(a) shows the discharge curves of the A-PPy/PPF composite at various discharge current densities,

the curves are almost linear in the whole potential range, whereas, Figure 6(b) shows the discharge curves of the M-PPy/PPF composite, and the curves are not as straight as Figure 6(a), which means A-PPy/PPF has good capacitive behavior.

Figure 7 shows the typical galvanostatic charge/discharge curve of PPY/PPF composite in 1.0M KCl electrolyte at a current density of 20 mA cm^{-2} . The capacitor cell based on A-PPy/PPF composite exhibits a triangular-shape charge/discharge curve, and a small iR drop is observed, indicating a highly conductive characteristic of the composite. However, the discharging curve of the capacitor fabricated from M-PPy/PPF composite shows two voltage stages in the ranges of 0.5 – 0.30 V and 0.3 V to -0.5 V, respectively. The former stage with a relatively short discharging duration is ascribed to EDL capacitance; while the latter stage with a much longer discharging duration is associated with the combination of EDL and Faradaic capacitances of PPY component. Yet, iR drop is much higher than that of A-PPy/PPF composite capacitor. This result reflects that the internal resistance of the latter device is much higher than that of the former. Low internal resistance is of

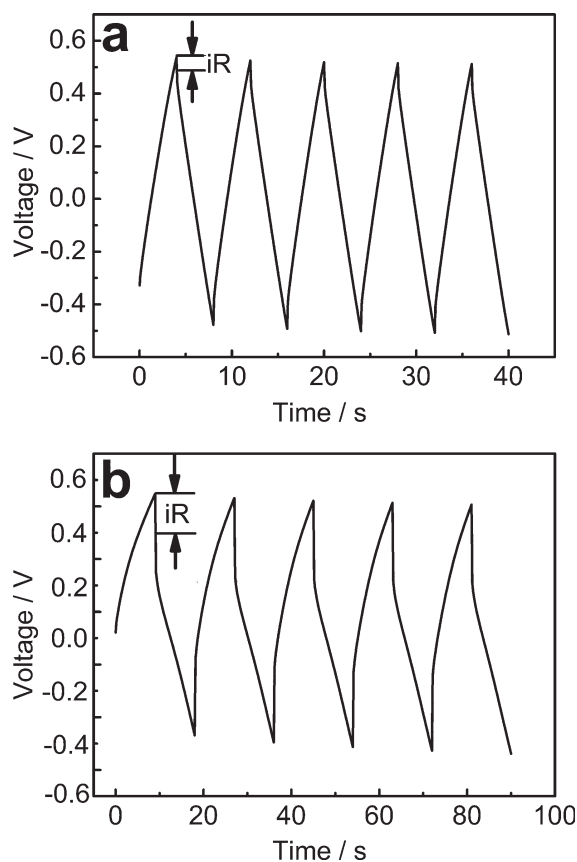


Figure 7 Charge/discharge curves of PPY/PPF composite at 20 mA cm^{-2} current density, (a) the A-PPy/PPF composite and (b) the M-PPy/PPF.

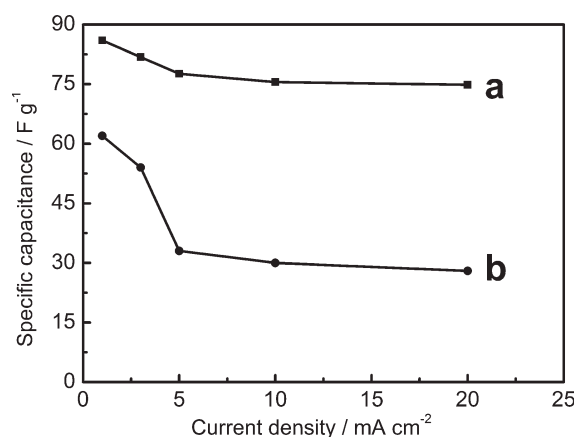


Figure 8 Discharge capacitance of PPy/PPF composite at various discharge current densities, a curve is the A-PPy/PPF composite and b curve is the M-PPy/PPF composite.

great importance in energy storing devices for less energy will be wasted to produce unwanted heat and electronic transportation during charging/discharging processes. Thus, A-PPy/PPF composite is more suitable for fabricating safe and power-saving capacitors compared with M-PPy/PPF composite.

The discharge capacitance may be calculated from the eq. (3):

$$C_m = I\Delta t / \Delta Vm \quad (3)$$

where C_m is the specific capacitance, I is the charge/discharge current, Δt is the discharge time, ΔV is the potential window, and m is the mass of active material. The specific capacitance calculated from the data in Figure 6 is shown in Figure 8. The specific capacitance decreases slightly when the current increases.

EIS is a useful experimental tool to characterize frequency response of the electrochemical capacitor.

EIS provides information on the charging/discharging progress, electronic/ionic conductivity of the electrode materials, and the equivalent series resistance. All the spectra exhibit a semicircle in the high-frequency region and a linear portion at the low-frequency region. The intercept of the semicircle in the high-frequency region at the real axis represents the internal resistance, which is related to the intrinsic electrical resistance of the active materials, the electrolyte resistance, and the contact resistance at the interface between the active material and current collector. The change in intercept is largely affected by the electrical resistance of the active materials because the other factors are under similar conditions.⁴³ Figure 9(a) represents the Nyquist plots obtained at open-circuit potentials for PPy/PPF composites. As pointed out before, a single semicircle in the high-frequency region and a straight line in the low-frequency region for both curves are observed. From the inset in Figure 9(a), a small semicircle is observed in the high-frequency region, which represents a parallel combination of the resistive and capacitive components. The charge-transfer resistance of A-PPy/PPF is smaller than that for M-PPy/PPF, which is an important factor in the fast redox systems such as electrochemical capacitor. A straight line can be seen in the low frequency, the straight line of A-PPy/PPF composite electrode leans more towards imaginary axis, indicating that it has better capacitive character. For electrochemical capacitors, the majority of their capacitance is only available at low frequency, so attention should be paid to the data in this range in the EIS spectra.⁴⁴ Figure 9(b) presents the conversion capacitance obtained from EIS of the PPy/PPF composites. The capacitance values are obtained from the following eq. (4)⁴⁵:

$$C_m = -1/2\pi mfZ'' \quad (4)$$

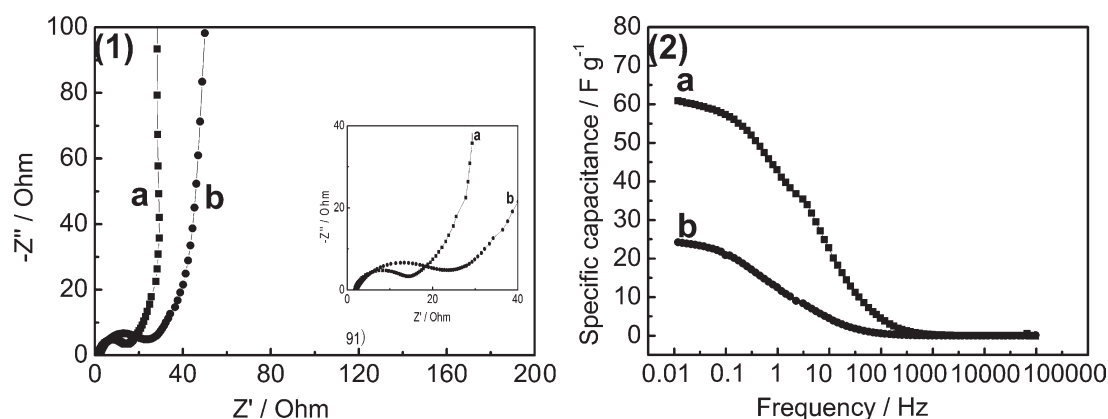


Figure 9 (1) Nyquist plot of the PPy/PPF composite. (2) The plots of capacitance versus frequency for the PPy/PPF composites, a curve is the A-PPy/PPF composite and b curve is the M-PPy/PPF composite.

Here, C_m is the specific capacitance, f is the frequency, Z'' is the imaginary part of EIS, and m is the mass of active material. When the frequency increases, the capacitance of all samples decreases, and at high-frequency region the capacitors behave like a pure resistance, which indicates that the electrolyte ions can not be doped or undoped into the matrix under high frequencies. It is found that A-PPy/PPF has a higher capacitance at low-frequency range compared with M-PPy/PPF, which is consistent with CV and charge/discharge data. It should be noted that the specific capacitance values of the samples at 0.01 Hz are deviated from those derived from CV and charge/discharge test, which is mainly due to the different testing systems applied.

CONCLUSIONS

The composite materials of PPy/PPF with various contents of PPy have been synthesized successfully *in situ* by chemical oxidation polymerization in the pyrrole vapor. And the presented PPy/PPF composite material is lightweight, flexible, and mechanically robust. The composite prepared from acetonitrile solution of oxidant exhibits the maximum conductivity at 8.0% PPy content, the specific capacitance of capacitor cell assembled by the A-PPy/PPF composite is approximately 72.5 F g^{-1} . Furthermore, electrochemical measurements show that the 8.0% A-PPy/PPF composite possesses excellent charge/discharge properties at high scan rate. The uses of these types of composite materials may be found in flexible energy storage devices.

References

- Arico, A. S.; Bruce, P.; Scrosati, B.; Tarascon, J. M.; Van Schalkwijk, W. *Nat Mater* 2005, 4, 366.
- Kotz, R.; Carlen, M. *Electrochim Acta* 2000, 45, 2483.
- Conway, B. E. *J Electrochem Soc* 1991, 138, 1539.
- Arbizzani, C.; Mastragostino, M.; Soavi, F. *J Power Sources* 2001, 100, 164.
- Sarangapani, S.; Tilak, B. V.; Chen, C. P. *J Electrochem Soc* 1996, 143, 3791.
- An, K. H.; Kim, W. S.; Park, Y. S.; Moon, J. M.; Bae, D. J.; Lim, S. C.; Lee, Y. S.; Lee, Y. H. *Adv Funct Mater* 2001, 11, 387.
- Wang, D. W.; Li, F.; Liu, M.; Lu, G. Q.; Cheng, H. M. *Angew Chem Int Ed* 2007, 47, 373.
- Zhang, H.; Cao, G. P.; Wang, Z. Y.; Yang, Y. S.; Shi, Z. J.; Gu, Z. N. *Electrochem Commun* 2008, 10, 1056.
- Kong, L. B.; Lang, J. W.; Liu, M.; Luo, Y. C.; Kang, L. *J Power Sources* 2009, 194, 1194.
- Nishide, H.; Oyaizu, K. *Science* 2008, 319, 737.
- Sugimoto, W.; Yokoshima, K.; Ohuchi, K.; Murakami, Y.; Takasu, Y. *J Electrochem Soc* 2006, 153, A255.
- Nam, K. T.; Kim, D. W.; Yoo, P. J.; Chiang, C. Y.; Meethong, N.; Hammond, P. T.; Chiang, Y. M.; Belcher, A. M. *Science* 2006, 312, 885.
- Frackowiak, E.; Bèguin, F. I. *Carbon* 2002, 40, 1775.
- Park, B. O.; Lokhande, C. D.; Park, H. S.; Jung, K. D.; Joo, O. S. *J Power Sources* 2004, 134, 148.
- Jang, J. H.; Han, S.; Hyeon, T.; Oh, S. M. *J Power Sources* 2003, 123, 79.
- Hu, C. C.; Chen, W. C. *Electrochim Acta* 2004, 49, 3469.
- Hu, C. C.; Chang, K. H. *J Power Sources* 2002, 112, 401.
- Hu, C. C.; Liu, M. J.; Chang, K. H. *J Power Sources* 2007, 163, 1126.
- Li, J.; Yang, Q. M.; Zhitomirsky, I. *J Power Sources* 2008, 185, 1569.
- Pandey, P. C.; Prakash, R. *J Electrochem Soc* 1998, 145, 999.
- Osaka, T.; Momma, T.; Ito, H.; Scrosati, B. *J Power Sources* 1997, 68, 392.
- Wang, J.; Xu, Y. L.; Chen, X.; Du, X. F. *J Power Sources* 2007, 163, 1120.
- Wu, Q. F.; He, K. X.; Mi, H. Y.; Xiao, X. G. *Mater Chem Phys* 2007, 101, 367.
- Chen, R.; Zhao, S. Z.; Han, G. Y.; Dong, J. H. *Mater Lett* 2008, 62, 4031.
- Han, G. Y.; Shi, G. Q. *Thin Solid Films* 2007, 515, 6986.
- Han, G. Y.; Shi, G. Q. *J Appl Polym Sci* 2007, 103, 1490.
- Han, G. Y.; Shi, G. Q. *J Electroanal Chem* 2004, 569, 169.
- Yao, T. J.; Lin, Q.; Zhang, K.; Zhao, D. F.; Lv, H.; Zhang, J. H.; Yang, B. *J Colloid Interface Sci* 2007, 315, 434.
- Najar, S. S.; Kaynak, A.; Foitzik, R. C. *Synth Met* 2007, 157, 1.
- Harlin, A.; Nousiainen, P.; Puolakka, A.; Pelto, J.; Sarlin, J. *J Mater Sci* 2005, 40, 5365.
- He, B. L.; Zhou, Y. K.; Dong, W. J.; Zhou, B.; Li, H. L. *Mater Sci Eng* 2004, A 374, 322.
- Jong-In, H.; In-Hyeong, Y.; Woon-Kie, P. *J Electrochem Soc* 2001, 148, A156.
- Huang, L. M.; Wen, T. C.; Gopalan, A. *Electrochim Acta* 2006, 51, 3469.
- Song, R. Y.; Park, J. H.; Sivakkumar, S. R.; Kim, S. H.; Ko, J. M.; Park, D. Y.; Jo, S. M.; Kim, D. Y. *J Power Sources* 2007, 166, 297.
- Mohammadi, A.; Ingnas, O.; Lundstrom, I. *J Electrochem Soc* 1986, 133, 947.
- Naegele, D.; Bittihn, R. *Solid State Ionics* 1988, 28, 983.
- Lee, J. Y.; Ong, L. H.; Chuah, G. K. *J Appl Electrochem* 1992, 22, 738.
- Rudge, A.; Davey, J.; Raistrick, I.; Gottesfeld, S.; Ferraris, J. P. *J Power Sources* 1994, 47, 89.
- Arbizzani, C.; Mastragostino, M.; Meneghello, L. *Electrochim Acta* 1996, 41, 21.
- Killian, J. G.; Coffey, B. M.; Gao, F.; Poehler, T. O.; Searson, P. C. *J Electrochem Soc* 1996, 143, 936.
- Song, H. K.; Palmore, G. T. R. *Adv Mater* 2006, 18, 1764.
- Grgur, B. N.; Gvozdenovic, M. M.; Stevanovic, J.; Jugovic, B. Z.; Marinovic, V. M. *Electrochim Acta* 2008, 53, 4627.
- Kim, D. W.; Noh, K. A.; Chun, J. H.; Kim, S. H.; Ko, J. M. *Solid State Ionics* 2001, 144, 329.
- Bakhtmatyuk, B. P.; Venhryna, B. Y.; Grygorchaka, I. I.; Micov, M. M. *J Power Sources* 2008, 180, 890.
- Ryu, K. S.; Lee, Y. G.; Kim, K. M.; Park, Y. J.; Hong, Y. S.; Wu, X. L.; Kang, M. G.; Park, N. G.; Song, R. Y.; Ko, J. M. *Synth Met* 2005, 153, 89.